Indian J. Phys. **79(2)**, 137-142 (2005)

AN INTERNATIONAL JOURNAL
IJP

Theoretical analysis of circular disk microstrip antenna with a slot

V Bhardwaj[2], Vijay Kumar Tiwari[1], D Bhatnagar[1*], J S Saini[1], P Kumar[3] and K B Sharma[2]
[1]Microwave Laboratory, Department of Physics, University of Rajasthan, Jaipur 302 004, Rajasthan, India
[2]Department of Physics, S S Jain Subodh PG College, Jaipur-302 004, Rajasthan, India
[3]Communication System Group, ISRO Satellite Center, Bangalore-560 017, Karnataka, India

E-mail : dbhatnagar_2000@rediffmail.com

Received 28 July 2004, accepted 16 December 2004

Abstract : The cavity model based modal expansion technique is applied to compute resonant frequency, input impedance, directivity and radiation efficiency of a general circular disk microstrip antenna having a narrow slot (CDMAS). The radiation performance of this circular disk antenna with a narrow slot ($\beta = 5°$) is found better in TM_{21} mode of excitation. The computed results show a fairly good agreement with simulated results obtained with commercial simulation software IE3D. An average deviations within 0.7%, 3.3%, 4.8% and 3.4% respectively, in resonant frequency, directivity, radiation efficiency and input impedance of this structures are recorded which validates this technique of treating proposed geometry.

Keywords : Microstrip antennas, cavity model, radiation patterns, input impedance.

PACS Nos. : 84.40.Ba, 75.50.Gg

1. Introduction

Planer circular disk antennas have been extensively used in variety of systems as low profile antennas [1–3]. However on every occasion, circular geometry may not be proved useful, particularly, when these radiators are required for conformal mounting on preexisting structures. Under geometrical constraints, other geometries are required to replace most commonly used rectangular and circular microstrip antenna geometries. Annular ring [4], gap open ring [5], annular sector antennas [6] and ring slot antennas [7] have been investigated by some workers but no serious effort on the analysis of circular disk microstrip antenna having a narrow slot (CDMAS) has been made. In this paper, an extensive theoretical formulation and analysis of CDMAS geometry with slot angle (β = 5°) is carried out in dominant mode of excitation by considering infinite ground plane dimensions. Expressions for fields inside the cavity are determined and hence, expressions for the far zone radiated fields are derived by using vector potential technique. Several of the computed results are validated with simulation results obtained with commercial simulation software IE3D.

2. Antenna geometry and coordinates system

Different workers have analyzed regular circular disk microstrip antennas in dominant mode of excitation. From different investigations, it has been realized that meandering of excited patch leads to a greatly lengthened current path for a fixed patch dimensions. This leads to lowered fundamental resonant frequencies and thus, a large antenna size reduction at a fixed operating frequency can be obtained. Considering this aspect, a narrow slot is inserted on the patch surface of a regular circular disk antenna. The feed arrangement is shown from the side view in Figure 1a. The patch geometry of radius a with slot angle β is assumed designed on a substrate with substrate thickness ($h << \lambda_0$), relative permittivity ε_r, loss tangent tan (δ) and having an infinite ground plane. The patch geometry is more clearly shown in the top view of patch in Figure 1b. The dimensions OA and OB of the slot are kept equal to the patch radius while slot angle between OA and OB is considered equal to β = 5°. For

*Corresponding Author

a regular circular disk antenna, the total radiation fields are normally determined from the knowledge of equivalent magnetic current sources associated with curved apertures but now in the present case, due to insertion of narrow slot, contributions of two equivalent magnetic current sources will have to be considered. These are (i) equivalent magnetic current sources associated with curved aperture M_ϕ and (ii) gap equivalent magnetic sources M_1

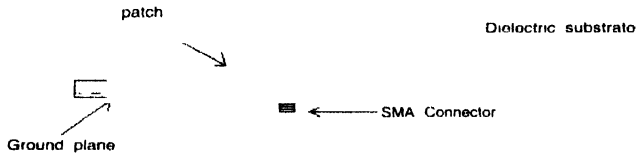

Figure 1a. Equivalent magnetic current sources of CDMAS geometry.

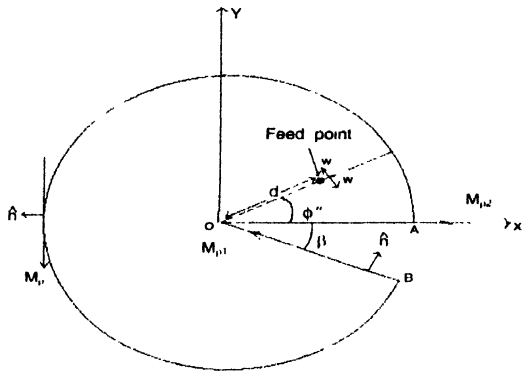

Figure 1b. The feed modeling of CDMAS geometry.

and M_2. In this way, the total path length of surface current will increase considerably.

Out of several available techniques, the cavity model-based modal expansion technique is adopted here to analyse present antenna geometry because this model is simple in application and provides reliable results. Later, the results with this technique are validated with the method of moment (MOM) based IE3D simulation software.

The region between the patch and ground plane is treated as a cavity bounded by magnetic wall along the edge of the patch and electric walls above and below. Many modal waves may get excited when a cable feeds such an antenna. The current density J due to coaxial line feed considered in this paper, can be represented by a cylindrical band of current flowing from the ground plane to the patch, plus an annular ring of magnetic current at the coaxial opening in the ground plane [1]. The later can be neglected with little error and former can be idealized by assuming that it is equivalent to a uniform current ribbon of some effective width $2w$, centered on the feed axis at a distance d from the center of the patch. The feed modeling of CDMAS geometry is shown in Figure 1b. The patch is excited in such a way that the input current at feed location (d, ϕ'') is

$$J = J_z(\phi')\frac{\delta(\rho - d)}{\rho}\hat{z} \tag{1}$$

with

$$J_z(\phi') = J \quad \phi'' - w < \phi' < \phi'' + w$$
$$= 0 \text{ elsewhere.}$$

Assuming eigen functions to be orthogonal, the solution of wave equation for E_z in the cavity with excitation current J_z in z direction, will be [8]

$$E_Z = j\omega\mu \sum_{\nu}\sum_{m} \frac{1}{\left(K^2 - K_{\nu m}^2\right)} \frac{\langle J_z \psi_{\nu m}\rangle}{\langle \psi_{\nu m}\psi_{\nu m}^*\rangle}\psi_{\nu m} \tag{2}$$

Here, $K_{\nu m}$ is the eigen values wave number (K) in the dielectric substrate given by

$$K = k_0\sqrt{\varepsilon_r\left(1 - j\tan(\delta)\right)} \tag{3}$$

The (m, ν)-th cavity mode $\psi_{\nu m}$ is given by

$$\psi_{\nu m} = J_\nu(K_{\nu m}\rho)\cos(\phi') \tag{4}$$

On applying this relation, different term of eq. (1) are determined as

$$\langle \psi_{\nu m}\psi_{\nu m}\rangle = \int_0^a \int_0^{(2\pi-\beta)} \int_0^h \left[J_\nu(K_{\nu m}\rho)\right]^2 \cos^2(\nu\phi')\rho d\rho d\phi' dz$$

$$= \frac{h}{4}\left[J_\nu(K_{\nu m}a)\right]^2 \left(a^2 - \frac{\nu}{K_{\nu m}^2}\right)$$

$$\times\left[(2\pi - \beta) + \frac{\sin[2\nu(2\pi - \beta)]}{2\nu}\right] \tag{5}$$

$$\langle J\psi_{\nu m}\rangle = \int_{\phi''-w}^{\phi''+w} \int_0^h J_\nu(\phi)\frac{J_\nu(K_{\nu m}d)}{\rho}\cos(\nu\phi')dd\phi' dz$$

$$= 2Jh\frac{\sin(\nu w)}{\nu}\cos(\nu\phi'')J_\nu(K_{\nu m}d) \tag{6}$$

On substituting eqs. (5) and (6) in equation (2), an expression of electric field component E_z inside the

cavity under the modified condition is obtained as

$$E_z = E_0 J_\nu (K_{\nu m}\rho)\cos(\nu\phi'), \tag{7}$$

with

$$E_0 = -j\omega\mu \sum\sum \times 2J \frac{\sin(\nu\, w)}{\nu}\cos(\nu\phi'')\, J_\nu(K_{\nu m}d)$$

$$\overline{(K^2 - K_{\nu m}{}^2)\frac{1}{4}\left[J_\nu(K_{\nu m}a)\right]^2\left[a^2 - \frac{\nu^2}{K_{\nu m}^2}\right]}$$

$$\times \left[(2\pi-\beta) + \frac{\sin[2\nu(2\pi-\beta)]}{2\nu}\right]. \tag{8}$$

Here, $J_\nu(K_{\nu m}\rho)$ is the cylindrical function of first kind of Bessel's function of order ν.

For a narrow slot $(2\pi - \beta) \sim 2\pi$,

therefore, $\nu \sim n / 2$, $(n = 1, 2, 3...)$ (9)

It may be noticed that for even values of n, expression of electric field component E_z of CDMAS, inside the cavity, shown by eq. (7), reduces to that for a circular patch antenna. An approximate value of $K_{\nu m}$ for axial modes ($m = 1$) can be obtained by assuming that mean length of strip line forming the radiator is a multiple of half wave length of microstrip line as in the case of a circular patch antenna [5].

The resonance frequency of CDMAS geometry is determined by

$$f_r = \frac{(K_{\nu m}a)\,c}{2\pi\, a_e\sqrt{\varepsilon_r}} \tag{10}$$

Here, $(K_{\nu m}a)$ is the m-th zero of the derivative of the Bessel function of order ν and a_e is the effective radius of patch that takes into account the fridge fields for CDMAS. To incorporate the effect of slot angle on the resonance frequency, the relation for effective radius of a circular disk antenna [1] is modified as

$$a_e = a\left[1+\left(\frac{(2\pi-\beta)}{2\pi}\right)\left(\frac{2h}{\pi a\varepsilon_r}\right)\left\{\ln\left(\frac{\pi a}{2h}\right)+1.7726\right\}\right]^{1/2} \tag{11}$$

The obtained results are shown in Table 1, which indicate that a nice agreement between computed and simulated resonance frequencies for CDMAS with ($\beta = 5°$) may be obtained in TM_{21} mode though a circular disk microstrip antenna without any slot provides better performance in TM_{11} mode of excitation [9].

Table 1. Radiation intensities and resonant frequencies of different CDMAS geometries in TM_{11} and TM_{21} modes.

Circular disk with different slot angles	Resonant frequency (GHz)		Max R-th (in dB)	
	TM_{11} mode	TM_{21} mode	TM_{11} mode	TM_{21} mode
0°	2.747	4.557	0	–13.67
5°	1.739	2.749	–5.595	–0.294
7.5°	1.740	2.749	–5.403	–0.147
10°	1.740	2.750	–5.209	0

a = 20 mm, ε_r = 2.32

By applying equivalence principle and image theory, components of equivalent magnetic current sources M associated with considered antenna are calculated. These are :

$$M_\phi = 2E_0 J_\nu(K_{\nu m}a)\cos(\nu\phi') \quad \text{at} \quad \rho = a,\ 0 < \phi > 2\pi, \tag{12}$$

$$M_{\rho 1} = 2E_0 J_\nu(K_{\nu m}\rho) \quad \text{at} \quad \phi = 0,\ 0 < \rho > a, \tag{13}$$

$$M_{\rho 2} = 2E_0 J_\nu(K_{\nu m}\rho)\cos[\nu(2\pi-\beta)]$$

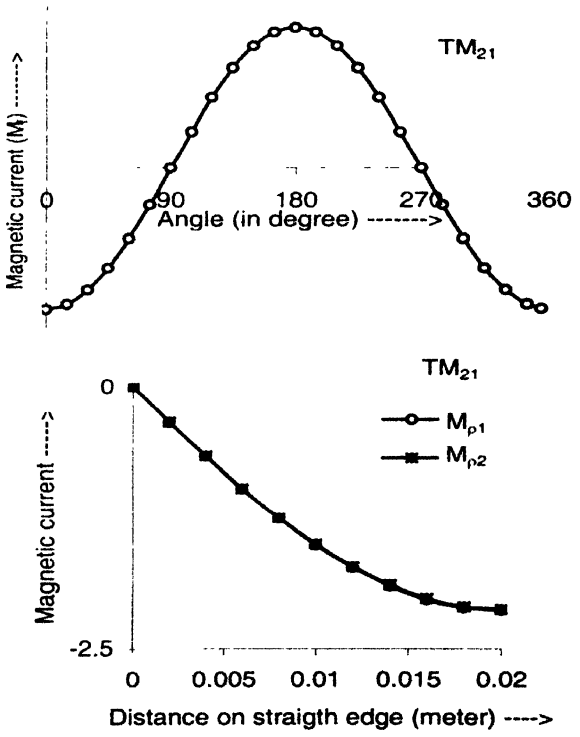

at $\phi = 2\pi,\ 0 < \rho > a$. (14)

The magnetic current distributions in TM_{21} mode of excitation are shown in Figures 2(a) and 2(b).

These magnetic current (M) distributions are then applied to compute vector potential F given by

$$' = \frac{\varepsilon_0}{4\pi}\iint M(r')\,\frac{e^{-jk_0|r-r'|}}{|r-r'|}\,ds'$$

which in turn, are applied under far field conditions

$$E_\theta = -j\omega\eta_0\left[F_\rho \sin(\phi'-\phi) + F_\phi \cos(\phi'-\phi)\right], \quad (15)$$

$$E_\phi = +j\omega\eta_0\left[F_\rho \cos(0)\cos(\phi'-\phi) - F_\phi \cos(\theta)\sin(\phi'-\phi)\right]. \quad (16)$$

The total field pattern factor of antenna in free space is obtained by using the relation

$$R_{th} = \left[|E_\theta|^2 + |E_\phi|^2\right]. \quad (17)$$

On substituting $\beta = 0$ and $\nu = n$, all the above-mentioned relations convert in those relations available for a regular circular disk microstrip antenna [1]. Using these relations, the variation of radiation intensity of antenna in TM_{21} is computed. The feed point is taken at one of the edge of the slot (OA) at $(d, \phi'' = 0)$.

The computed ($\phi = 0°$) and ($\phi = 90°$) plane patterns of CDMAS geometry are compared with the simulated

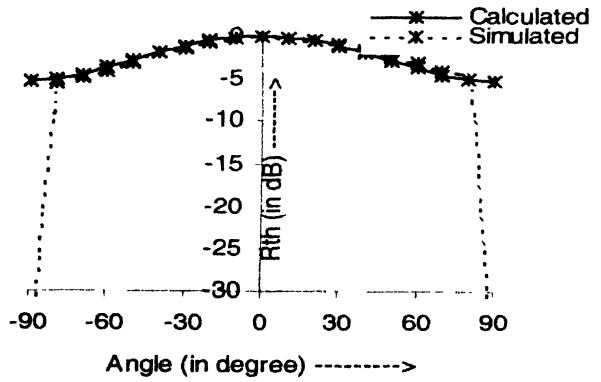

Figure 3. Calculated and simulated ($\phi = 0°$) plane radiation patterns of CDMAS geometry in its dominant mode of excitation.

results and are shown in Figures 3 and 4 respectively, in dominant TM_{21} mode. For these calculations, feed location and filamentary current (J_z) are taken as (d, 0) and unity, respectively. The computed relative radiation intensity results in different modes are shown in Figure 5, which indicates that a circular disk antenna with a slot radiates more power in TM_{21} mode of excitation.

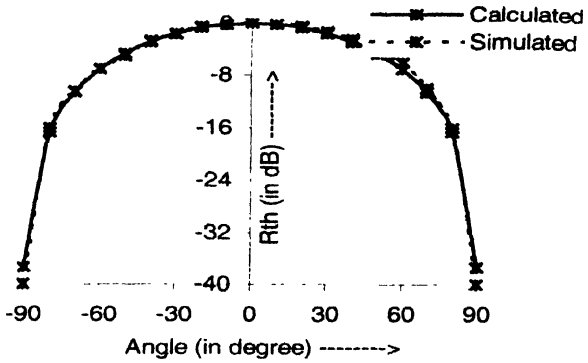

Figure 4. Calculated and simulated ($\phi = 90°$) plane radiation patterns CDMAS geometry in its dominant mode of excitation.

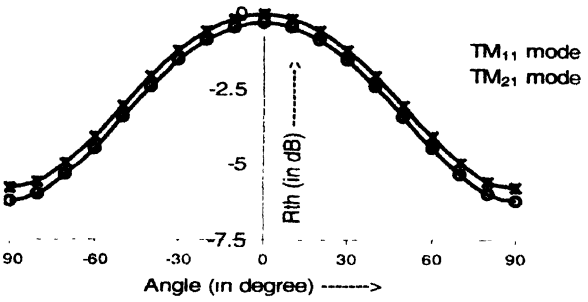

Figure 5. Computed relative radiation intensity results in different modes

Input impedance of 50Ω probe-fed CDMAS geometries is determined following method adopted in [9]

$$Z_{in} = R + jX = \frac{V}{I} = \frac{E_{av}h}{I} \quad (18)$$

Here, E_{av} is the average value of the electric field at the feed point and I is the total current and are defined by

$$E_{av} = \frac{1}{2w}\int_{\pi-w}^{\pi+w} E_z(d,\phi)\,d\phi \quad (19)$$

and $$I = -J(2wd). \quad (20)$$

On applying these relations, real part of input impedance and return loss of CDMAS geometry ($\beta = 5°$) are computed in its dominant mode between the frequency range 2.40 GHz to 2.90 GHz and are compared with simulation results in Figures 6 and 7, respectively. The resonance peak obtained from our theoretical analysis is at 2.632 GHz, which is found to be 2.65 GHz from the simulation analysis. This small difference of 0.7% in resonance frequencies may be tolerated since both analysis modes have their own working limitations. A difference of 3.4% between computed and simulated values of real

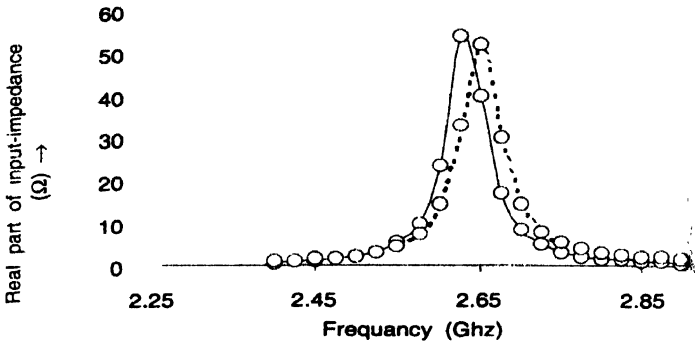

Figure 6. Variation of input impedance of a CDMAS geometry ($\beta = 5°$) wi frequency in TM_{21} mode. Feed ($d = 5.85$ mm, $\phi'' = 0°$).

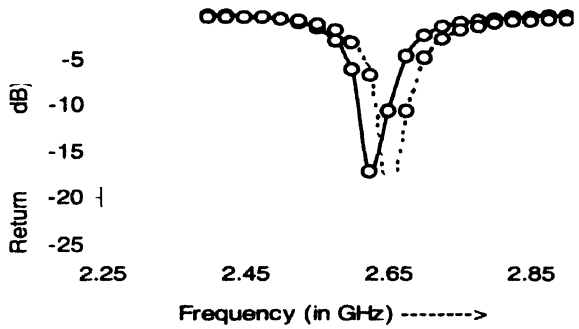

Figure 7. Variation of calculated and simulated return losses of a CDMAS geometry ($\beta = 5°$) in TM_{21} mode.

input impedance for circular disk antenna with slot ($\beta = 5°$) at its resonance frequency is recorded. The calculated and simulated E and H-plane directive gains of CDMAS geometry with $\beta = 5°$ are shown in Figure 8.

The computed directivity of this antenna is 7.02 dB, which is 3.3% less than the simulated directivity (7.25 dB) of this antenna. The directivity, quality factor, radiation efficiency and input impedance for CDMAS geometry in TM_{21} mode of excitation antenna are also calculated and compared with simulation results in Table 2. A difference of 4.8% between computed and simulated radiation efficiencies is recorded.

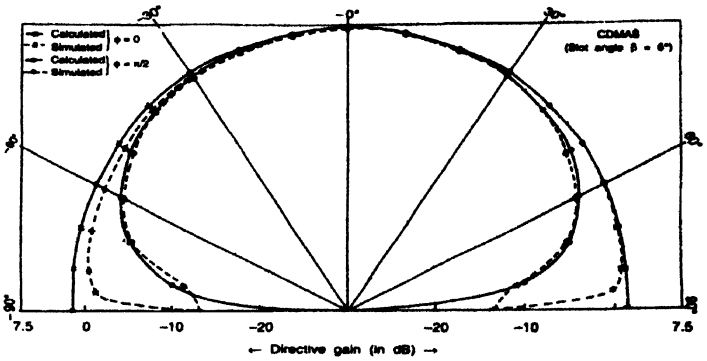

Figure 8. Calculated and simulated ($\phi = 0$) and ($\phi = 90°$) plane gain of a CDMAS geometry ($\beta = 5°$) in TM_{21} mode.

3. Conclusions

The analysis carried out in this paper is thoroughly validated and the results suggest that the present technique may be applied to treat a circular disk antenna carrying a narrow slot to a reasonably good accuracy. The overall radiation performances of a normal circular disk antenna and CDMAS geometry are quite comparable; hence, an appropriate CDMAS geometry may be mounted on pre-existing structures where mounting of normal circular geometry is difficult.

Table 2. Different antenna parameters of CDMAS geometries in dominant modes.

Circular disk with different slot angles	Dominant mode (n, m)	Quality factor (Q_t)	Directivity (in dB)		Radiation efficiency (%)		Real part of input impedance (Ω)	
		Calculated	Calculated	Simulated	Calculated	Simulated	Calculated	Simulated
0°	TM_{11}	46.85	7.27	–	93.95	–	46.83*	55.00*
5°	TM_{21}	46.04	7.24	7.0	94.05	89.5	48.27+	63.25+
7.5°	TM_{21}	45.63	7.22	–	94.11	–	50.11	–
10°	TM_{21}	45.22	7.2	–	94.16	-	50.11	–

*Feed point ($d = 5.70$ mm, $\phi'' = 0$)

+Feed point ($d = 5.85$ mm, $\phi'' = 0$)

Acknowledgments

The authors are thankful to ISRO, Bangalore for granting a research project to work. Authors are also thankful to Dr. S Raniwala for sparing computation facilities from his DST sponsored project.

References

[1] J R James and P S Hall *Handbook of Microstrip Antenna* (London : Peter Peregrinus) (1989)

[2] N C Karmakar IEEE *Trans. Antenna and Propagation* **50** 1076 (2002)

[3] H How, C Vittoria, L C Kempel and K T Trott *IEEE Trans. Antenna and Propagation* **49** 393 (2001)

[4] Y X Guo, K M Luk and K F Lee *IEEE Trans. Antenna and Propagation* **49** 19 (2001)

[5] M A Sultan *IEEE Trans. Antenna and Propagation* **37** 137 (1989)

[6] M A Sultan and V K Tripathi *IEEE Trans. Antenna and Propagation* **38** 265 (1990)

[7] L K Wong, C C Haung and W S Chen *IEEE Trans. Antenna and Propagation* **50** 75 (2002)

[8] Y T Lo, D Solomon and W F Richards *IEEE Trans. Antenna and Propagation* **27** 137 (1979)

[9] R Garg, P Bhartiya, I Bahl and A Ittipiboon *Microstrip Antenna Design Handbook* (Boston : Artech House) (2001)

[10] C A Balanis *Antenna Theory Analysis and Design*, (New York John Wiley & Sons Inc.) (1982)

[11] K R Carver and J M Mink *IEEE Trans. Antenna and Propagation* **29** 2 (1981)